Journal of Materials and Environmental Sciences
ISSN : 2028-2508

Copyright © 2017,
University of Mohammed Premier
Oujda Morocco

JMES, 2017 Volume 8, Issue 5, Page 1676-1689

http://www.jmaterenvironsci.com/

Cinnamon essential oil as a novel eco-friendly corrosion inhibitor of copper in 0.5 M Sulfuric Acid medium

K. Dahmani[1], M. Galai[2,*], M. Cherkaoui[1], A. El hasnaoui[3], A. El Hessni[3]

1.Laboratory of Materials, Electrochemistry and Environment, Faculty of Science, Ibn Tofail University, Kénitra, Morocco
2.Laboratory of Materials Engineering and Environment: Modeling and Application, Faculty of Science, University Ibn Tofail BP. 133-14000, Kenitra, Morocco
3.Laboratoire de Neuroendocrinologie, Biotechnologie et Génétique, Faculty of Science, Ibn Tofail University, Kénitra, Morocco

Received 26 Oct 2016,
Revised 22 Feb 2017,
Accepted 27 Feb 2017

Keywords

- Cinnamon essential oil;
- Green corrosion inhibitor;
- Copper;
- H_2SO_4;

M.Galai
galaimouhsine@gmail.com
+212 6 77 23 56 95

Abstract
The oil of Cinnamon essential (CiO), analyzed by gas chromatography (GC) and gas chromatography–mass spectrometry (GC–MS) was made. The analyzed oils consist mainly Trans-cinnamaldehyde (46.30%), δ-cadinene (8.16%) and β-Cubebene (5.20%) being the major constituents, on the corrosion of copper in aqueous 0.5 M sulfuric acid studied by electrochemical impedance spectroscopy (EIS) and potentiodynamic polarization. EIS and polarization measurements showed that the dissolution process of copper occurs under diffusion control. Potentiodynamic polarization curves indicated that the essential oil extract behaves as cathodic-type inhibitor. The corrosion rates of copper and the inhibition efficiencies of the extract were calculated. The results obtained show that the extract solution of the essential oil could serve as an effective inhibitor for the corrosion of copper in sulphuric acid media.

1. Introduction

Due to its excellent thermal conductivity and good mechanical workability, copper is a material commonly used in heating and cooling systems. Scale and corrosion products have a negative effect on heat transfer, and they cause a decrease in heating efficiency of the equipment, which is why periodic descaling and cleaning in sulphuric acid (or hydrochloric acid) pickling solutions are necessary. Corrosion inhibitors effectively eliminate the undesirable destructive effect and prevent metal dissolution. Most of commercially available pickling inhibitors are toxic compounds that should be replaced with new environmentally friendly inhibitors [1]. The use of copper corrosion inhibitors in such conditions is necessary since no protective passive layer can be expected. The possibility of the copper corrosion prevention in different aqueous solutions has attracted many researchers so until now numerous possible inhibitors have been investigated. These studies reported that there are a number of organic and inorganic compounds which can do that for the corrosion of copper [2-6]. It is noticed that presence of heteroatoms such as nitrogen, sulphur, phosphorous in the
organic compound molecule improves its action as copper corrosion inhibitor. Amongst these organic compounds and their derivatives such as azoles [7, 8], amino acids [9] and many others, but these compounds are highly toxic. Recently, the research is oriented to the development of green corrosion inhibitors, compounds with good inhibition efficiency but low risk of environmental pollution. Plant extracts have attracted attention in the field of corrosion inhibition for many decades. As natural products, they are a source of non-toxic, eco-friendly, readily available and renewable inhibitors for preventing metal corrosion [10].
In continuation of our work on testing the cinnamon essential oils as corrosion inhibitors of electrochemical copper coating [11], we have studied the inhibition efficiency of extract of essential oil for copper corrosion in 0.5 M Sulfuric Acid solution using electrochemical techniques and weight loss measurements. The effect of temperature on the corrosion behavior of copper in 0.5 M H2SO4 without and with the extract essential oil was investigated. In addition, adsorption of extract on a copper surface was studied to examine basic information about the interaction between the green inhibitor and the metal surface. Finally, to complete this study, the adsorption mechanism of the extract molecules was proposed and is discussed.

2. Experimental section

2.1 Material preparation

Cinnamon is a spice (Figure1) obtained from the inner bark of several trees from the genus Cinnamomum that is used in both sweet and savoury foods. The term "cinnamon" also refers to its mid-brown colour. While Cinnamomum verum is sometimes considered to be "true cinnamon", most cinnamon in international commerce is derived from related species, which are also referred to as "cassia" to distinguish them from "true cinnamon". Cinnamon is the name for perhaps a dozen species of trees and the commercial spice products that some of them produce. All are members of the genus Cinnamomum in the family Lauraceae produced in China. Only a few of them are grown commercially for spice.

Figure 1: Cinnamon sticks and Powder

Cinnamon was procured from local market and *Cinnamon* oil (CO) was extracted by hydrodistillation in a Clevenger-type apparatus at 100 °C for 5h and finally the oil was isolated and kept in a dark glass in the refrigerator until required for further use. The plant is identified by Botany Laboratory and Plant Protection, Faculty of Sciences, Ibn Tofail University, Morocco.

2.2. Preparation of working electrodes

The commercial copper used in this study had the following chemical composition (by weight %): 0.019 P, <0.001 Fe, <0.001 As, <0.001 Mn, <0.002Sb, <0.001 Al, 0.009 Sn, 0.003 Ni, 0.015 Pb, <0.005 Ag, <0.001 Bi, <0.001 S, <0.005 C, the balance being Cu. Coupons were cut into 2.5 cm × 2.0 cm × 0.05 cm dimensions used for weight loss measurements.

2.3. Solution preparation

The test solutions were prepared from analytical grade reagent and distilled water: 98% H_2SO_4.

2.4. Potentiodynamic polarization results

For electrochemical measurements, the electrolysis cell was a borrosilcate glass (Pyrex®) cylinder closed by a cap with five apertures. Three of them were used for the electrode insertions. The working electrode was pressure-fitted into a polytetrafluoroethylene holder (PTFE) exposing only 1cm^2 of area to the solution. Platinum and saturated calomel were used as counter and reference electrode (SCE), respectively. All potentials were measured against the last electrode.

The potentiodynamic polarization curves were recorded by changing the electrode potential automatically from negative values to positive values versus E_{corr} using a Potentiostat/ Galvanostat type PGZ 100, at a scan rate of 1 mV/s after 1 h of immersion time until reaching steady state. The test solution was thermostatically controlled at 298 K in air atmosphere without bubbling.To evaluate corrosion kinetic parameters, a fitting by Stern-Geary equation was used.To do so, the overall current density values, i, were considered as the sum of two contributions, anodic and cathodic current i_a and i_c, respectively. For the potential domain not too far from the open circuit potential, it may be considered that both processes followed the Tafel law [12]. Thus, it can be derived from equation (1):

$$i = i_a + i_c = i_{corr}\left\{\exp\left[b_a \times \left(E - E_{corr}\right)\right] - \exp\left[b_c \times \left(E - E_{corr}\right)\right]\right\} \quad (1)$$

where i_{corr} is the corrosion current density (A cm^{-2}), b_a and b_c are the Tafel constants of anodic and cathodic reactions (V^{-1}), respectively. These constants are linked to the Tafel slopes β (V/dec) in usual logarithmic scale given by equation (2):

$$\beta = \frac{\ln 10}{b} = \frac{2.303}{b} \quad (2)$$

The corrosion parameters were then evaluated by means of nonlinear least square method by applying equation (1) using Origin software. However, for this calculation, the potential range applied was limited to ±0.100V around E_{corr}, else a significant systematic divergence was sometimes observed for both anodic and cathodic branches.

The corrosion inhibition efficiency is evaluated from the corrosion current densities values using the relationship (3):

$$\eta_{PP} = \frac{i^{0}_{corr} - i_{corr}}{i^{0}_{corr}} \times 100 \quad (3)$$

The surface coverage values (θ) have been obtained from polarization curves for various concentrations of inhibitor using the following equation [13]:

$$\theta = 1 - \frac{i_{corr}}{i^{0}_{corr}} \quad (4)$$

where i^{0}_{corr} and i_{corr} are the corrosion current densities values without and with inhibitor, respectively.

The electrochemical impedance spectroscopy measurements were carried out using a transfer function analyzer (VoltaLab PGZ 100), with a small amplitude a.c. signal (10 mV rms), over a frequency domain from 100 kHz to 100 mHz with five points per decade. The EIS diagrams were done in the Nyquist representation. The results were then analyzed in terms of an equivalent electrical circuit using Bouckamp program [14].

The inhibiting efficiency derived from EIS, η_{EIS} is also added in section 3.3, and calculated using the following equation (5):

$$\eta_{EIS} = \frac{R_{ct} - R^{0}_{ct}}{R_{ct}} \times 100 \quad (5)$$

where R^{0}_{ct} and R_{ct} are the charge transfer resistance values in the absence and in the presence of inhibitor, respectively.

In order to ensure reproducibility, all experiments were repeated three times. The evaluated inaccuracy did not exceed 10 %.

3. Results and discussions

3.1. GC-MS analysis

The essential oils were analyzed by gas chromatography coupled to mass spectrometry (GC-MS) using the Thermo Fisher apparatus in UATRS - cnrst, Rabat, Morocco. It consisted of chromatograph Trace GC Ultra type coupled to a mass spectrometer Polaris Q type. The capillary column used is a DB5 30 m long, 0.25mm diameter and 0.25 µm thick. The oven temperature was programmed at 333 K for 1 minute and gradually rose up to 573 K at the 303 K / min for the remaining 1 minute. The carrier gas used was helium with a flow rate of 1 ml/min. The sample was injected with a volume of 1 µl. Mass spectra of different compounds identified are recognized and affirmed by using the database NIST. Retention indices of the various compounds were compared by referring to the literature [15]. Regarding the chromatographic analysis of Cinnamon essential oils by GC/MS, we found that 38 compounds represent 86.21% of CiO with Trans-cinnamaldehyde (46.30%), δ-cadinene (8.16%) and β-Cubebene (5.20%) being the major constituents and these molecules are presented in table 2

These compounds were thought to be good candidates for corrosion inhibition due to the presence of Trans-cinnamaldehyde in the Cinnamon essential oils extract. Trans-cinnamaldehyde was found to be a very effective and environment-friendly acid corrosion inhibitor by Hugel [16]. Since then, it has been extensively used in the oilfield industry, and many attempts have been made in order to elucidate its inhibiting mechanism [17–19] .The table 3 shows the other works on this oil but the copper and H_2SO_4 are never studied in the presence of the Cinnamon essential oils extract.

Table 1: Composition of Cinnamon essential oils extraction

Retention Time (min)	*Compounds*	*Indicative Value %*
3,01	α-phellandrène	0.01
3,06	D 3-Carene	0.02
3,10	α-terpinene	0.01
3,16	p-cymene	0.21
3,20	Limonene	0.17
3,23	1,8-cineole	0.13
3,29	Phenylacetaldehyde	0.02
3,42	γ-terpinene	0.05
3,47	acetophenone	0.09
3,65	Terpinolene	0.07
3,71	trans β-ocimene	0.04
3,80	α-Thujone	0.11
3,88	β-Thujone	0.23
4,00	Benzene terbutyl	0.28
4,10	2-methyl benzofuran	0.02
4,12	Camphor	0.28
4,23	hydrocinnamaldehyde	1.64
4,28	Borneol	0.42
4,36	Terpinen-4-ol	0.07
4,46	α-terpinol	0.20
4,50	Estragole	Tr
4,69	Cis cinnamaldehyde	1.62
4,86	Cuminicaldehyde	1.27
5,28	**Transcinnamaldehyde**	**46.30**
5,72	Eugenole	0.12
5,82	α–copaene	1.36
5,89	**β–Cubebene**	**5.20**
5,96	β-selinene	0.43
5,98	Valancene	0.38
6,02	Viridiflorene	0.62
6,23	α-Logipinene	0.29
6,52	α-murolene	3.97
6,68	γ-cadinene	4.84
6,83	**δ-cadinene**	**8.16**
7,48	Cubenol	1.69
7,57	T-Cadinol	4.58
7,75	Cadalene	1.21
8,22	Benzyl benzoate	0.10
Total		**86.21**

Table 2: Major constituent of cinnamon essential oil extract

Name		*Trans-cinnamaldehyde*	*δ-cadinene*	*β-Cubebene*
Structure	Compound Structure	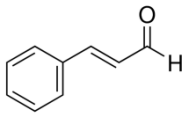	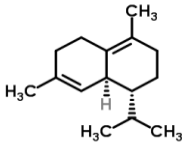	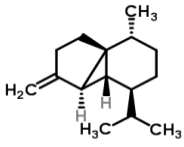
	Molecular Formula	C_9H_8O	$C_{15}H_{24}$	$C_{15}H_{24}$
Properties	Formula weight (g/mol)	132.16	204.35	204.35
	Solubility in water	Water Solubility		

Table 3: Revue bibliography on works that studied the mechanism of inhibition in presence of cinnamon essential oil extract

Sample number	*Metal / Alloy*	*Medium*	*Reference*
1	API J55	15% HCl	[20]
2	Carbon steel	20% and 28% HCl	[21]
3	Duplex stainless steel	20% and 28% HCl	[21]
4	Superaustenitic steels ($27Cr_{31}Ni_3Mo$)	20% and 28% HCl	[21]
5	Superaustenitic steels ($19Cr_{25}Ni_4Mo$)	20% and 28% HCl	[21]
6	AISI 1018 carbon steel	6.0 M HCl	[22]
7	Steel	1.0 M HCl	[23]
8	High-Ni ferrous alloy (Incoloy 825)	15% HCl	[24]
9	13Cr-L80 (Uniloy-420)	15% HCl	[24]
10	N80 steels	15% HCl	[24]

3.2 Potentiodynamic polarization curves

The dissolution kinetics of copper in sulfuric acid has been studied byseveral researchers [25-28], According to these authors, the anodic dissolution of copper takes place in two continuous steps

$$Cu - e^{-} \overset{K_1/K_{-1}}{\longleftrightarrow} Cu\ (I)_{ads} \qquad \textit{(fast step)}$$

$$Cu\ (I)_{ads} - e^{-} \overset{K_2/K_{-2}}{\longleftrightarrow} Cu\ (II) \qquad \textit{(the rate-determining step)}$$

where $Cu(I)_{ads}$ is an adsorbed species at the copper surface and does not diffuse into the bulk solution. It is inferred from the reaction model that the steady-state polarization curve of copper should give an apparent Tafel region of 40 mV/decade slope, which has been confirmed by some authors [28-30].

Figure 2 shows a set of polarization curves for the copper electrode measured in 0.5 M H_2SO_4 solution alone and in the presence of various concentrations of Cinnamon essential oils.

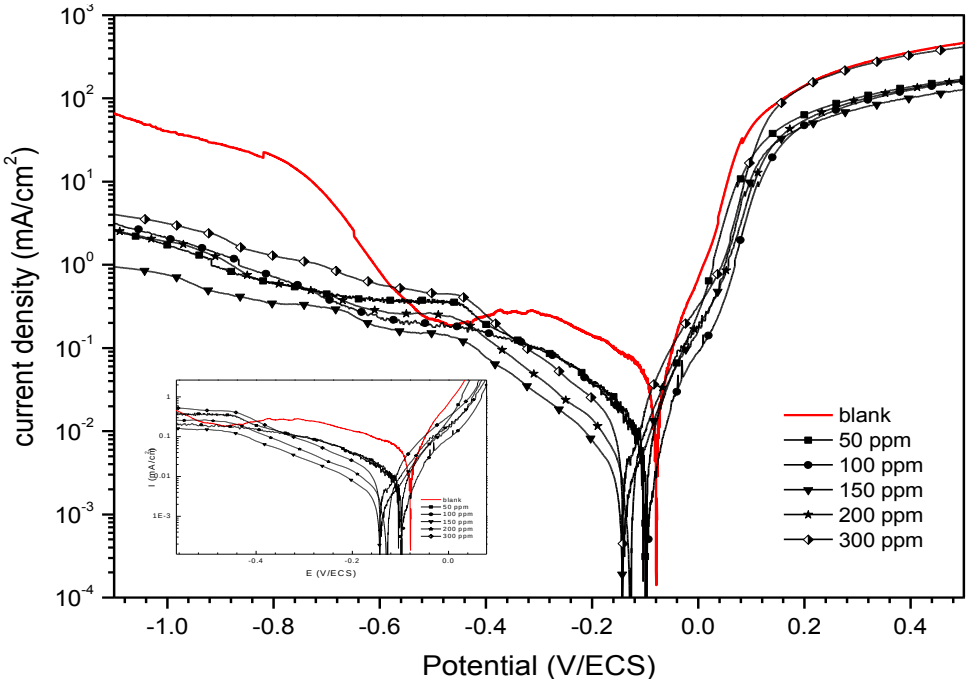

Figure 2: Potentiodynamic polarization curves for copper in 0.5 M H_2SO_4 in the absence and presence of various concentrations of Cinnamon essential oil extract.

In each case, the polarization measurement was carried out after the corrosion potential reached an approximately stable value to ensure the reaction system was in the steady state. By comparing polarization curves in the absence and presence of Cinnamon essential oils extract, it is observed that the increase in Cinnamon essential oils concentration shifted the open circuit potential in the negative direction and a slight lowering of both the anodic and cathodic current densities.

Kinetic parameters such as E_{corr}, corrosion current density (j_{corr}), cathodic (b_c) and anodic (b_a) Tafel slopes and inhibition efficiency *(η_{pp} %)* are listed in Table 4. The addition of Cinnamon essential oils led to a change of anodic and cathodic Tafel slopes besides decreasing both currents. Table 4 shows that the *IE* increases with the Cinnamon essential oils concentration up to a maximum (89.62%) in a concentration of 150ppm and then it decreases.

Table 4: Electrochemical data from the potentiodynamic curves carried out on copper at 298 K in 0.5 M H_2SO_4 without and with different concentrations of Cinnamon essential oil during 1 H of immersion.

Inh.	*Conc ppm*	E_{corr} (mV/SCE)	i_{corr} ($\mu A\ cm^{-2}$)	*Tafel slopes (mV dec^{-1})* $-\beta_c$	β_a	η_{pp} %	θ
Blank	0	-79	29.0	204	59.0	-	-
CiO	50	-105	4.5	150	63.0	84.48	0.445
	100	-97	3.7	132	40.7	87.24	0.872
	150	-144	3.3	121	57.0	89.62	0.896
	200	-128	3.5	108	64.0	88.93	0.889
	300	-139	6.0	137	51.0	79.31	0.793

3.3. Electrochemical Impedance Spectroscopy (EIS)

In practical electrode system, the impedance spectra obtained often were depressed semi-circles with their center below the real axis. This kind of phenomenon is known as the dispersing effect. Considering that the impedance of a double-layer did not behavior as an ideal capacitor in the presence of dispersing effect, the *CPE* was used as a substitute for capacitor in the equivalent circuit, to fit more accurately the impedance behavior of electric double-layer. The *CPE* is a special element, whose admittance value is a function of the angular frequency *(ω)*, and whose phase is independent of the frequency. Its admittance and impedance are respectively, expressed as: [33].

$$Z_{CPE} = Y^{-1}\,(j\omega)^{n} \qquad (6)$$

Where *Y* is the magnitude of the *CPE*, *j* is the imaginary number *($j^2=-1$)*, *α* is the phase angle of *CPE* and *$n=\alpha/(\pi/2)$*.The factor *n* is an adjustable parameter that usually lies between 0 and 1. The *CPE* describes an ideal capacitor when *n=1*. Values of *α* are usually related to the roughness of the electrode surface. The smaller value of α is due to the higher the surface roughness [32].

Figures 3 and 5 show the Nyquist and bode plots respectively, recorded for copper in 0.5M H_2SO_4 solution with different concentration of Cinnamon essential oil extract. It is also noted that this plots consisted of two badly separated loops. The one at high frequency was attributed to the adsorbed species resistance due to adsorption of the molecules inhibitor and all other accumulated products. Conversely, the one at low frequency was usually attributed to the double layer capacitance and the charge transfer resistance.

The charge transfer resistance, R_t, values are calculated from the difference of impedance at lower and higher frequencies [32,34]. To obtain the double layer capacitance *(C_{dl})*, the frequency at which the imaginary component of the impedance is maximum *($-Z''_{max}$)* is found and C_{dl} values are obtained from the equation [31]:

$$f(-Z''_{max}) = {}^{1}/_{(2\pi C_{dl} R_t)} \qquad (7)$$

The polarization resistance R_p value was used to calculate the inhibition efficiency (η_{EIS}%) of Cinnamon essential oil extract for copper at different concentrations.

The Nyquist impedance spectrum for copper in 0.5 M H_2SO_4 was analyzed by the equivalent circuit shown in Figure 4(b). R_s represents the solution resistance, R_{ct} the charge-transfer resistance[37]. All impedance spectra obtained from the copper electrode exposed for 1 h to the Cinnamon essential oil extract containing H_2SO_4 solutions were analyzed by the equivalent circuit in Figure 4 (a).

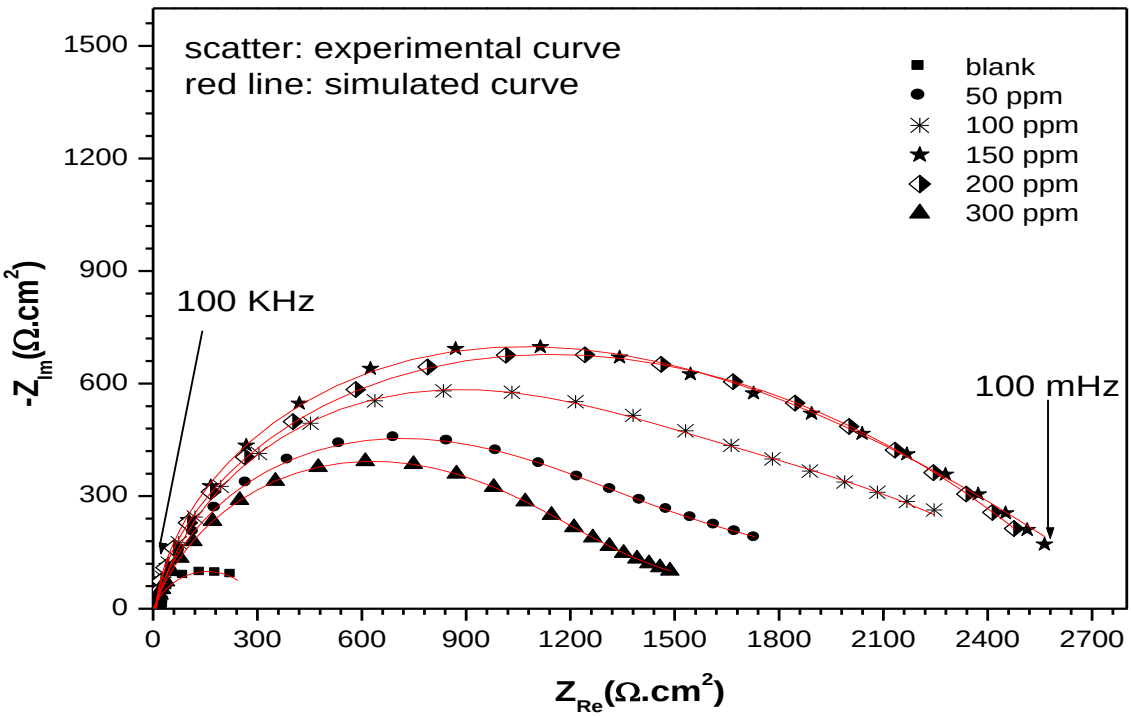

Figure 3: Nyquist plots for copper in 0.5 M H_2SO_4 solution in the absence and presence of various concentrations of Cinnamon essential oil extract at 298 K :comparison of experimental (scatter) and fitting (red line) data.

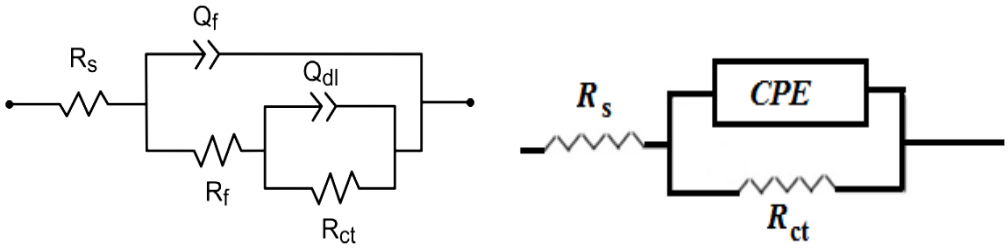

(a) (b)

Figure 4: Electrical equivalent circuit model used to fit the experimental impedance data for copper in (a) presence and (b) absence of Cinnamon essential oil extract

Compared with copper in 0.5 M H_2SO_4 (blank solution), the impedance display of the copper in the Cinnamon essential oil-containing solutions greatly changed in shape and size. Taking that, even if the electrode was immersed in H_2SO_4 solution containing 150 ppm of Cinnamon essential oil extract for only 60 min, the presence of Cinnamon essential oil led to changes of impedance behavior in the following aspect: diameter of the R_p obviously increased, from349Ω cm^2 in the absence of Cinnamon essential oil extract *(CiO)* to more than 2736 Ω cm^2in the presence of *(CiO)*.The impedance parameters derived from these investigation is given in Table 5. It is found that, as the Cinnamon essential oil extract concentrations increase, the R_p values increase, but the C_{dl} values tend to decrease. The decrease in the C_{dl} value is due to the adsorption of Cinnamon essential oil extract on the metal surface. This decrease can be caused by a decrease in the local dielectric constant and /or the increase in the thickness of the double layer. It shows that the molecules of inhibitor act by adsorption at the solution-metal interface [35]. The capacity of film containing the inhibitor is given by the formula:

$$C_{dl} = {}^{\varepsilon\varepsilon_0}/_{d} \qquad (8)$$

where d is the thickness of the organic coating, ε is the relative permittivity, and ε_0 is the permittivity of vacuum. Therefore, the decrease in the values of C_{dl} shows that, the adsorption layer formed by Cinnamon essential oil extract on the metal surface is stable and thick [36].

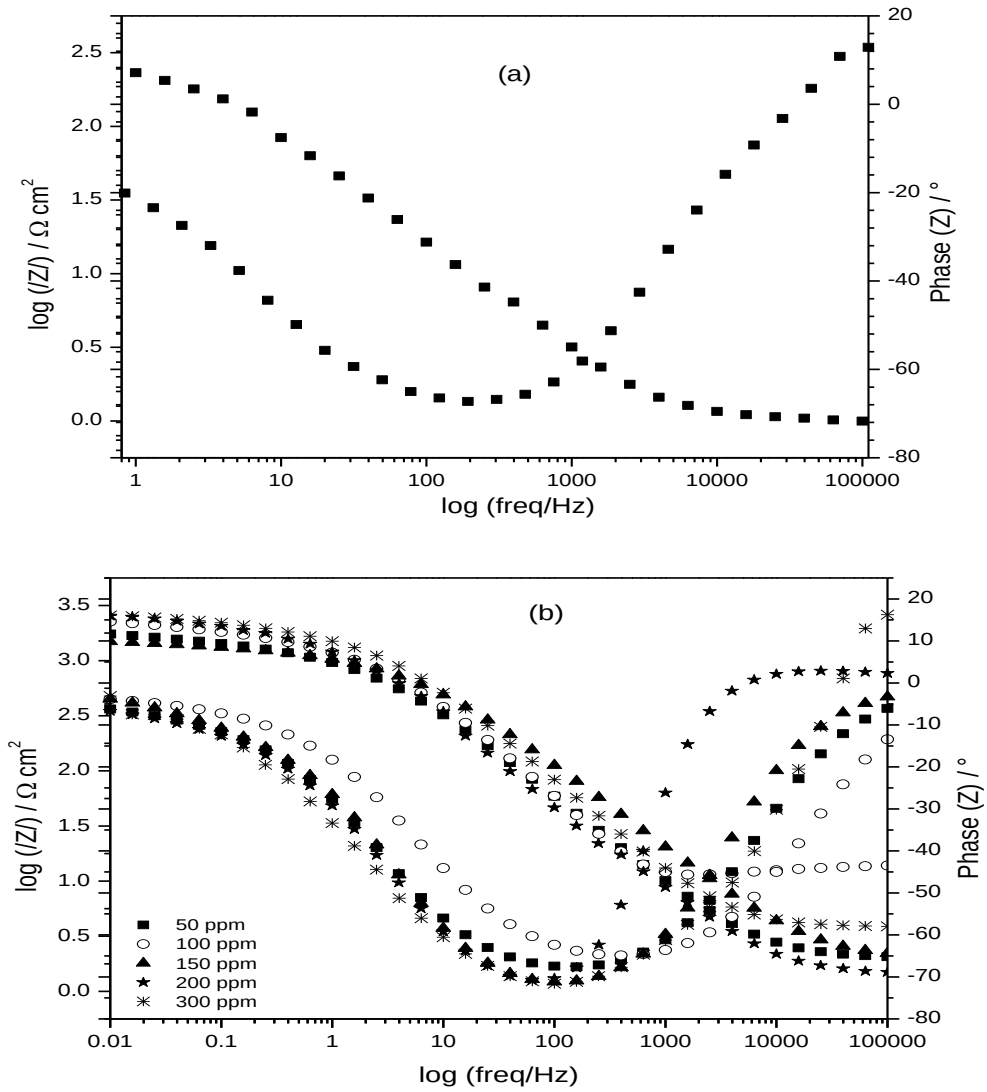

Figure 5: Nyquist and Bode diagrams plots for copper in 0.5 M H_2SO_4 solution (a) without and (b) with various concentrations of Cinnamon essential oil extract.

Table 5: Electrochemical impedance parameters and inhibition efficiency for copper in 0.5 M H_2SO_4 solution without and with different concentration CiO at 298 K

Inhibitor	*Conc.*	R_s	Q_f	n_f	R_f	Q_{ct}	n_{ct}	R_{ct}	R_p	*E%*
	Ppm	*Ω.cm²*	*μFcm⁻²*		*Ω.cm²*	*μF cm⁻²*		*Ω cm²*	*Ωcm⁻²*	
Blank	0	0.7	-	-	-	475	0.72	350	349	-
CiO	50	2.0	93	0.32	846	973	0.80	1367	2213	84.23
	100	2.5	72	0.48	1109	517	0.84	1497	2606	86.61
	150	2.0	49	0.53	1265	685	0.85	1471	2736	87.24
	200	2.0	82	0.49	1256	570	0.83	1455	2711	87.13
	300	2.0	54	0.18	420	236	0.78	1205	1625	78.52

3.4. Adsorption isotherm

The adsorptive behavior of a corrosion inhibitor is an important part of its study. The adsorption of inhibitors is governed by the residual charge on the surface of the metal and by the nature and chemical structure of inhibitor. Two main type of adsorption of organic inhibitor on a metal surface are physical or electrostatic and chemisorptions. The chemisorption involves the share or transfer of charge from the molecules to the surface to

form a coordinate type bound. Electron transfer is typical for transition metals having vacant low-energy electron orbital. As for inhibitors, the electron transfer can be expected with compounds having relatively loosely bound electrons. The most frequently used isotherms are the Langmuir isotherm, the Freundlich isotherm and the Temkin isotherm [37,38]. All these isotherms are of the general form:

$$f(\theta, x) \times e^{-2\alpha\theta} = KC \qquad (9)$$

where *f (θ,x)* is the configurational factor which depends upon the physical model and the assumptions underlying the derivation of the isotherm, θ the surface coverage, *C* the inhibitor concentration in the bulk solution, α the molecular interaction and *K* is adsorption constant.

Table 6 shows the most commonly used isotherms for studying the adsorption mechanism of an inhibitor on a metal electrode surface [39–47]. The meaning of the parameters in the table is as follows: k is the equilibrium binding constant of the adsorption below reactions

$$Cu + Inh \rightleftarrows Cu(Inh)_{ads}$$

$$Cu(Inh)_{ads} \rightleftarrows Cu^{n+} + ne^{-} + Inh$$

given by $k = (1/55.5)\exp(-\Delta G^0_{ads}/RT)$, the value 55.5 is the water concentration in the solution expressed in mol×l^{-1}; *R* is the gas constant (8.314 JK^{-1} mol^{-1}); *T* is the absolute temperature; ΔG^0_{ads} is the adsorption energy; $Cu(Inh)_{ads}$is a reaction intermediate; *f* is the interaction term parameter (*f*> 0 lateral attraction between adsorbed organic molecules and *f*< 0 repulsion between adsorbed molecules); χ is the number of water molecules replaced by one molecule of organic inhibitor (also referred to as the size ratio parameter)

$$Inh_{aqu} + \chi H_2O_{ads} \rightleftarrows Inh_{ads} + \chi H_2O_{aqu}$$

where Inh_{aqu} is the inhibitor in the aqueous phase and χH_2O_{ads} is the number of water molecules adsorbed on the copper surface. χ is assumed to be independent of the coverage or charge on the electrode.

Table 6 : Adsorption isotherms the most used

Author	*Isotherm*	*Eqn.*	*Réf.*
Langmuir	$kc = \frac{\theta}{1-\theta}$	*(10)*	[39]
Frumkin	$kc = \frac{\theta}{1-\theta}\exp(-f\theta)$	*(11)*	[40]
Hill-de Boer	$kc = \frac{\theta}{1-\theta}\exp\left(\frac{\theta}{1-\theta}\right)exp(-f\theta)$	*(12)*	[41,42]
Parsons	$kc = \frac{\theta}{1-\theta}\exp\left[\frac{2-\theta}{(1-\theta)^2}\right](-f\theta)$	*(13)*	[43]
Damaskin- Batrakov	$kc = \frac{\theta}{(1-\theta)^{\chi}}\exp(-f\theta)$	*(14)*	[44]
Kastening-Holleck	$kc = \frac{\theta}{\chi(1-\theta)^{\chi}}\left(1-\theta+\frac{\theta}{\chi}\right)^{(\chi-1)}\exp(-f\theta)$	*(15)*	[45]
Flory-Huggins	$kc = \frac{\theta}{\chi(1-\theta)^{\chi}}$	*(16)*	[45]
Dhar-Flory-Huggins	$kc = \frac{\theta}{(1-\theta)^{\chi}\exp(\chi-1)}$	*(17)*	[45]
Bockris-Swinkels	$kc = \frac{\theta}{(1-\theta)^{\chi}} \times \frac{[\theta+\chi(1-\theta)]^{(\chi-1)}}{\chi^{\chi}}$	*(18)*	[46]
El-Awady-Abd-El-Nabey-Aziz	$(kc)^{y} = \left(\frac{\theta}{1-\theta}\right)$	*(19)*	[47]

Finally in Table 6, y is defined as a thermodynamic/kinetic model (from a mechanistic kinetic point of view) and represents the number of inhibitor molecules occupying a given active site. Values of $1/y$ greater than unity imply the formation of multilayers of the inhibitor on the metal surface. Values of $1/y$ less than unity, however, mean that a given inhibitor will occupy more than one active site. The parameter c is the inhibitor concentration.
Finally, θ is the degree of coverage of the copper surface by adsorbed inhibitor. The θ value was obtained using the expression
In this study the Langmuir adsorption isotherm (Eqn. 10) was found. This isotherm is:

$$\theta/_{1-\theta} = AC \times e^{-2\alpha\theta} = KC \qquad (10)$$

The above equation can be simplified as:

$$C/_{\theta} = C + 1/_{K} \qquad (20)$$

The degree of surface coverage (θ) can readily be calculated from Equations (10) to (20). That degree is numerically identical to the value of percentage inhibition efficiency. Where C is the concentration of the inhibitor and K_{ads} represent the adsorption equilibrium constant. The plots of C/θ versus C yield a straight line (correlation coefficients R^2equal 0.99984) proving that experimental results are in good agreement with Langmuir adsorption isotherm (Figure 6). The value of K_{ads} is found as for CiO, K_{ads}=332.2 l mol^{-1}. The increasing value of K_{ads} reflects the increasing adsorption capability, due to structural formation, on the metal surface [47].

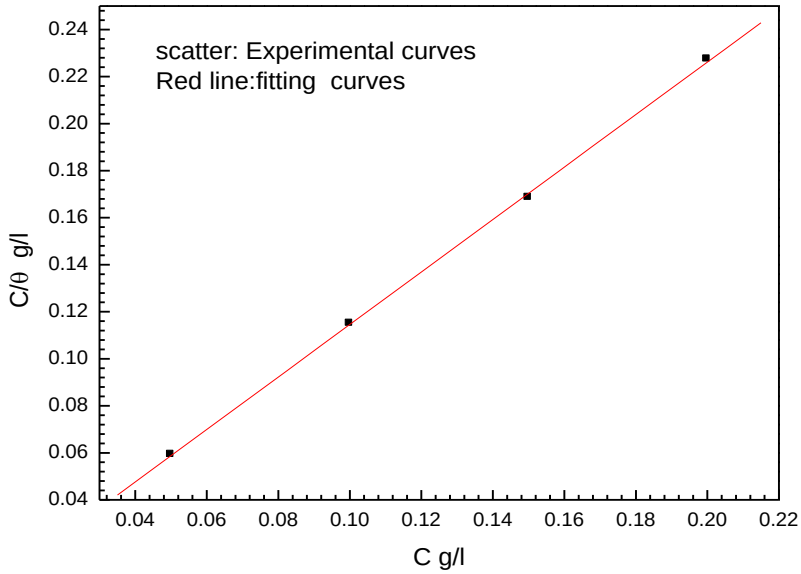

Figure 6: Plot of the Langmuir adsorption isotherm of Cinnamon essential oil extract on the copper surface at 298 K

The relation between the adsorption constant (K_{ads}) and adsorption free energy (ΔG^0_{ads}) is known as:

$$K_{ads} = \left(\frac{1}{55.55}\right) e^{-\Delta G_0/RT} \qquad (21)$$

Where R is the universal gas constant and T is the absolute temperature. On the basis of characterization of Cinnamon essential oil, we postulate that the major constituents act together by adsorption to ensure inhibition. Then, the inhibition is regarded as intermolecular synergistic effect of the various components of essential oil. It is adequately recommended to not determine ΔGads values since the mechanism of adsorption remains unknown[48]
The polarization curves in Figure 2 have shown that CiO inhibited the cathodic reaction. The impedance spectra for the copper in the CiO-containing solutions at the corrosion potentials did not display new low frequency capacitive (or inductive) loops in addition to the well-known high frequency semicircle. Thus, we can draw a conclusion that CiO is very good inhibitor for copper corrosion in sulfuric acid.
The inhibitive action is realized by the geometric coverage of Trans-cinnamaldehyde on the copper surface. In this case, IE may be considered as the surface coverage (θ) by the surfactant molecules on the copper surface[49].

3.5. Effect of temperature

The effect of temperature on the inhibited acid–metal reaction is highly complex, because many changes occur on the metal surface such as rapid etching and desorption of inhibitor and the inhibitor itself many undergo decomposition and/or rearrangement.

The change of the corrosion process rate with the temperature increase was studied in 0.5 M H_2SO_4, both in the absence and in the presence of Cinnamon essential oil extract. We were interested in exploring the activation energy of the corrosion process and the thermodynamic functions of adsorption of CiO oil extract. This was accomplished by investigating the temperature dependence of the corrosion current, obtained using Tafel extrapolation method. Some of the polarisation curves for mild steel electrode in 0.5 M H_2SO_4 in the absence and presence of 150 ppm of CiO in the temperature range 298 K to 328 K are given in Figures 7 and 8, respectively. The polarisation exhibits Tafel behaviour.

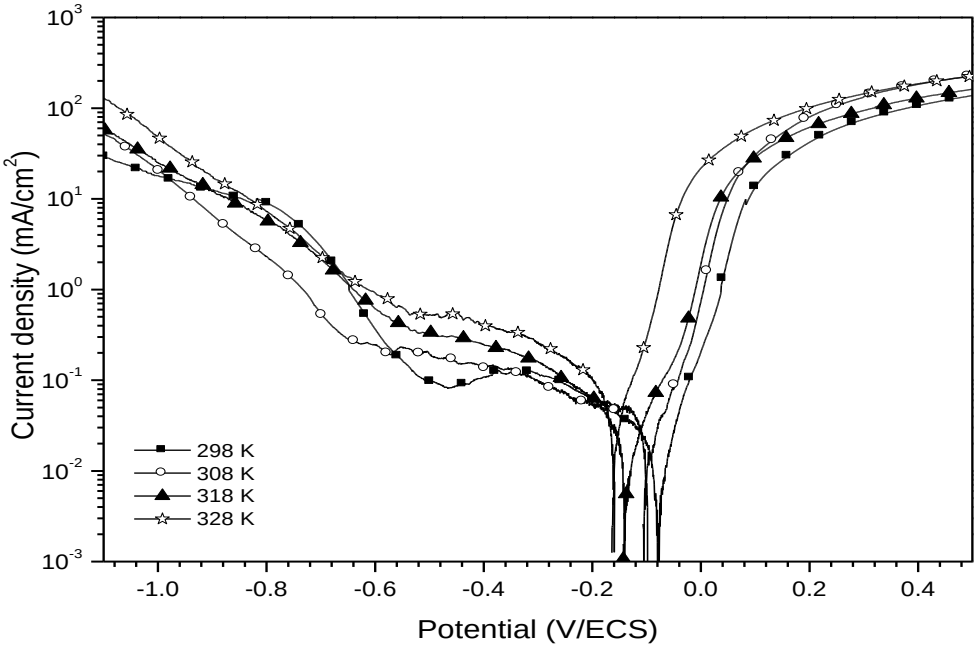

Figure 7: Potentiodynamic polarization curves for copper in 0.5M H_2SO_4 without inhibitor at different temperature.

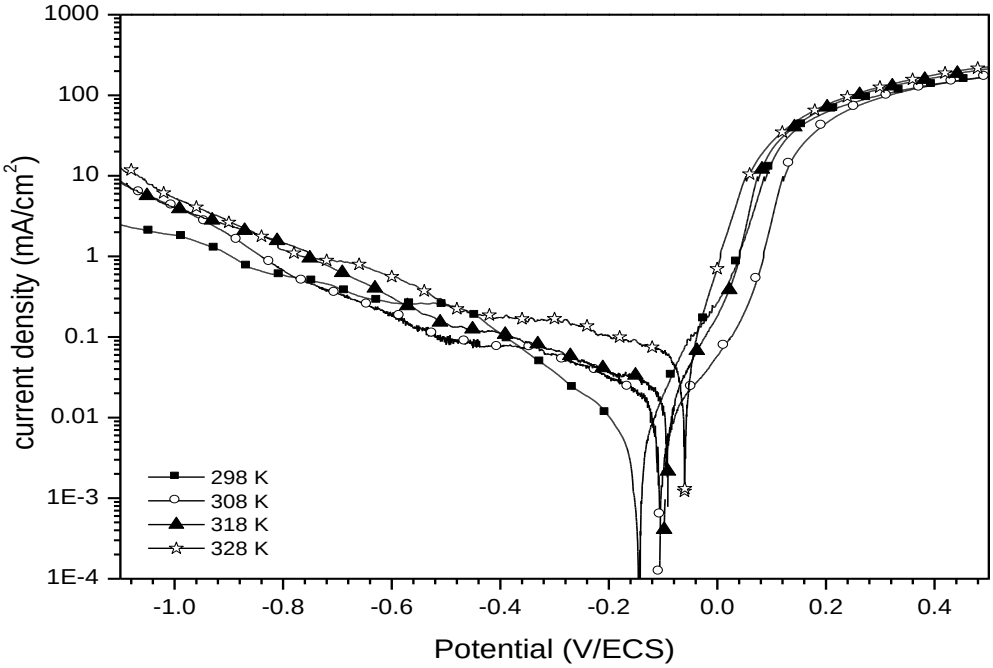

Figure 8: Potentiodynamic polarization curves for copper in 0.5M H_2SO_4 with 150 ppm of CiO at different temperature.

Table 7 : Electrochemical parameters and the corresponding inhibition efficiencies at various temperature studied of copper in 0.5M H_2SO_4 in absence and presence 150 ppm of CiO.

Compounds	*Temperature K*	*-E_{corr} mV/ECS*	*I_{corr} µA/cm²*	*-β_c mV*	*β_a mV*	*E %*
Blank (0.5 H_2SO_4)	298	79	29.0	204	59	-
	308	105	35.0	328	64	-
	318	142	56.0	164	77	-
	328	166	77.0	182	52	-
0.5 M H_2SO_4 with 150 ppm of CiO	298	144	3.3	121	57	88.62
	308	106	5.0	251	61	85.71
	318	94	10.0	205	78	82.14
	328	60	18.0	332	85	76.62

The kinetic parameters determined by computer fitting are listed in Table 8. It can be noted first that, once again, the cathodic reaction could only be modeled by the kinetic law corresponding to a mixed activation diffusion control. Secondly, it can be seen from figure 8 that increasing the temperature increased the current density of the potentiodynamic polarization curves. This is more clearly illustrated in Table 7 by the variations of i_{corr} with temperature, from 29.0 µA cm^{-2} at 298 K to 77.0 µA cm^{-2} at 328 K. The dependence of the corrosion rate on temperature can be expressed by the Arrhenius equation:

$$i_{corr} = Aexp\left(-{}^{E_a}/_{RT}\right) \quad (22)$$

where $i_{corr}$is the corrosion current density, A is the frequency factor, E_a is the activation energy of the copper corrosion reaction, T is the absolute temperature and R the universal gas constant (8.314 J mol^{-1} K^{-1}). The obtained Arrhenius plot *Ln i_{corr} vs. 1000/T* is given in figure 9. It is compared to that of copper in 0.5 M H_2SO_4 solution without inhibitor, drawn using the E_a value of 27.5 kJ mol^{-1} given in previous work [50] .

The experimental curve obtained with the Cinnamon essential oil extract corresponds approximately to a straight line and the E_a value can be determined from the slope of this line. The fitting of this curve with a straight line gave a value of 46.80 kJ mol^{-1} for the activation energy E_a of the corrosion process with 150 ppm of inhibitor. This value is significantly higher than that of 27.50 kJ mol^{-1} obtained previously for copper without inhibitor (and used for drawing the corresponding line in figure 10), which explains why the variations of i_{corr} are more pronounced in the presence of the inhibitor. This effect can be quantified by computing the inhibition efficiency at each temperature. The results, given in Table 7, show that η decreases when the temperature increases, from 89% at 298 K to 77% at 328 K.

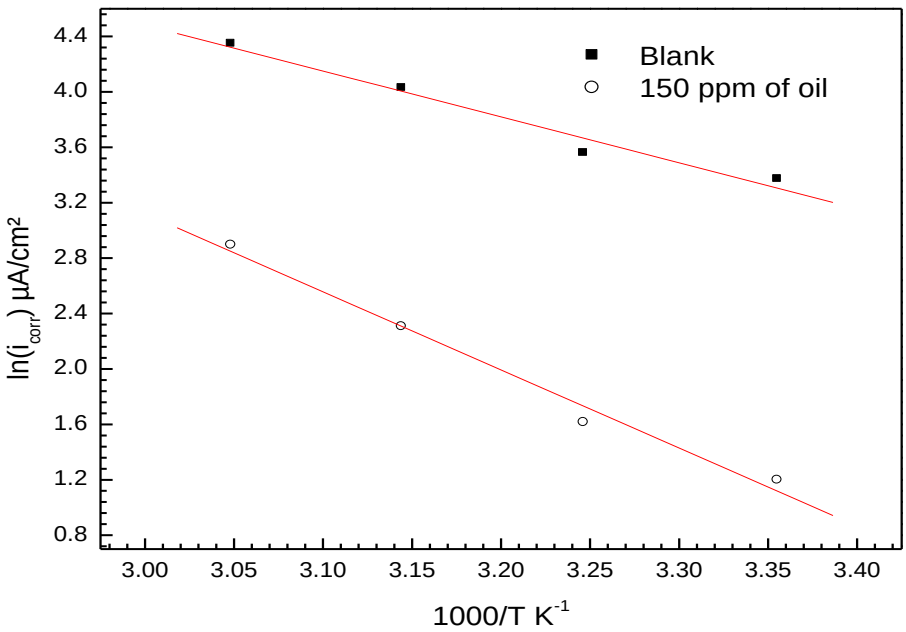

Figure 9: Arrhenius plots of copper in 0.5 M H_2SO_4 without and with 150 ppm of CiO.

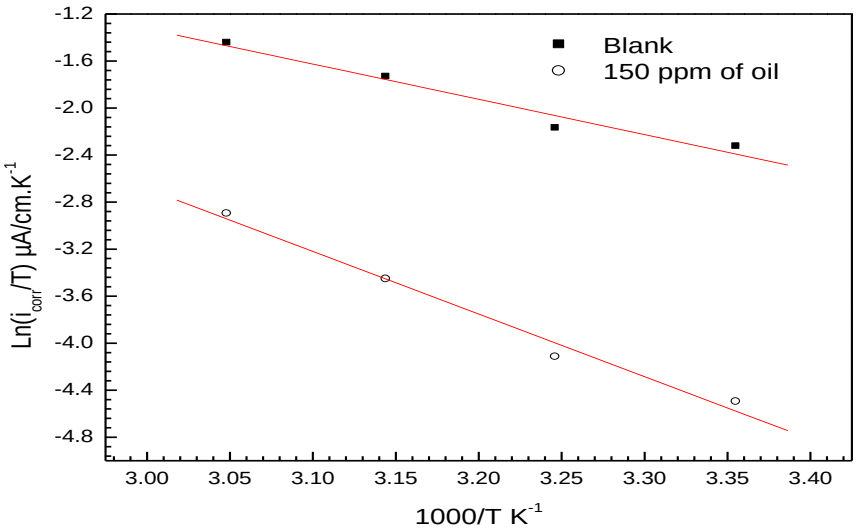

Figure 10: Arrhenius plots of Ln(i_{corr}/T) versus 1000/T for copper in 0.5M H2SO4 without and with 150 ppm of CiO

Table 8: The values of activation parameters E_a, ΔH_a^* and ΔS_a^* for copper in 0.5 M H_2SO_4 in the absence and presence of 150 ppm of CiO.

Compounds	E_a(kJ mol^{-1})	ΔH_a^* (kJ mol^{-1})	ΔS_a^* (J mol^{-1} K^{-1})
Blank solution	27.50	25.00	-134
150 ppm of CiO	46.80	44.30	-87.1

An increase of the corrosion activation energy in the presence of inhibitor, associated with a decrease in inhibition efficiency with increasing temperature, is frequently interpreted as due to the formation of an adsorption film of physical nature, i.e. involving electrostatic interactions with the metal surface [51,52]. Conversely, a chemisorption mechanism corresponds to an increase in inhibition efficiency with temperature and a lower activation energy in the presence of the inhibitor [53,54].

Our results suggest a predominant physisorption of the inhibiting species. Actually, it has been proposed that physisorbed molecules are bound to the metal at cathodic sites and mainly inhibit the corrosion process by hindering the cathodic reaction.

Moreover, it can also be deduced that the positive signs of the enthalpies ΔH_a^* reflect the endothermic nature of the copper dissolution process. Indeed, the increase in the enthalpy of activation in tha case of presence of inhibitor corresponds to a decrease in the dissolution of the metal.

Conclusion

From the above results and discussion, the following conclusions can be drawn:

- The IE increases with the Cinnamon essential oils concentration up to a maximum (89.62%) in a concentration of 150 ppm and then it decreases
- The concentration dependence of the inhibition efficiency calculated from electrochemical impedance spectroscopy and polarization curves are in good agreement.
- Based on the polarization results, the investigated CiO acts predominantly as an cathodic-type inhibitor.
- Adsorption of CiO on the copper surface in 0.5 M H_2SO_4 obeys the Langmuir adsorption isotherm model.
- The thermodynamic parameters of activation and adsorption are calculated, from this study the adsorption mechanism of CiO is physisorption.

References

1. Stupnisek-Lisac E., Gazivoda A., Madzarac M., *ElectrochimicaActa*. 47 (2002) 4189.
2. Liao P.Yu, D. M., Luo Y. B., Chen Z. G., *Corros.* 59 (2003) 314.
3. Qafsaoui W., Blanc C., Pebere N., Takenouti H., Srhiri A., Mankowski G., *Electrochim. Acta.* 47 (2002) 4339.
4. Zhang D.Q., Gao L.X., Zhou G.D., *Appl. Electrochem.* 33 (2003) 361.
5. Zhang D.Q., Gao L.X., Zhou G.D., *Corros. Sci.* 46 (2004) 3031.
6. Zhang D.Q., Gao L.X., Zhou G.D., *Appl. Surf. Sci*. 225 (2004) 287.
7. Sherif E.M., Park S.M., *Electrochim. Acta.* 51 (2006) 6556.

8. Sherif E.M., Park S., *Electrochim. Acta.* 51 (2006) 4665.
9. Matos J.B., Pereira L.P., Agostinho S.M.L., Barcia O.E., Cordeiro G.G.O., Elia E.D., *Electroanal. Chem.* 570 (2004) 91.
10. Chauhan L.R., Gunasekaran G., *Corros. Sci.* 49 (2007) 1143.
11. Dahmani K., Galai M., Elhasnaoui A., Temmar B., El Hessni A., Cherkaoui M., *Der Pharma Chemica.* 7 (2015) 566.
12. Stern M., Geary A. L., *J. Electrochem. Soc.* 104 (1957) 56.
13. AbdelAal M. S., Radwan S., El Saied A., *Br. Corros. J.* 18(1983) 2.
14. Williamson K. L., Minard R. D., *K. M. Masters Macroscale and Microscale Organic Experiments,* 5th Ed. 2007.
15. Hochmuth D., *Scientific consulting Terpenoids library list*.
16. Hugel G., *Corrosion inhibitors: study of their activity mechanism, in: 1st European Symp. Corros. Inh., Ferrara, Italy,* 1960.
17. Growcock F.B., Frenier W.W., *J. Electrochem. Soc.* 135 (1988) 817.
18. Growcock F.B., Lopp V.R., *Corrosion*. 44 (1988) 248.
19. Growcock F.B., Lopp V.R., Jasinski R.J., *J. Electrochem. Soc.* 135 (1988) 823.
20. Growcock F.B., Frenier W.W., *J. Electrochem. Soc.* 135 (1988) 817.
21. Trabanelli G., Zucchi F., Brunoro G., *Materials and corrosion* 39(1988) 589.
22. Hugel, G., *Corrosion Inhibitors—Study of their Activity Mechanism, in 1st European Symposium on Corrosion Inhibitors, Ferrara, Italy, U. of Ferrara,* 1960.
23. Growcock F. B.,Frenier W. W., *J. Electrochem. Soc.* 135(1988) 817.
24. Cabelloa G., Funkhouser G. P., Cassidy J., Kiser C. E., Lane J., Cuesta A.,*ElectrochimicaActa*.97 (2013) 1.
25. Smyrl W. H., *in Comprehensive Treatise of Electrochemistry, Vol*. 4, *p.* 116, *Plenum Press, New York* (1981)
26. Mattsson E. Bockris J. O'M., *Trans. Faraday Soc*.55 (1959) 1586.
27. Cordeiro G. G. O., Barcia O. E., Mattos O. R., *Electrochim. Acta.* 38 (1993) 319.
28. Wang D. K. Y., Coller B. A. W., Macfarlane D. R., *Electrochim. Acta.* 38 (1993) 2121.
29. CabanR.,Chapman T. W., *J. Electrochem. Soc.* 124 (1977) 1371.
30. Hurlen T., Ottesen G., Staurset A.,*Electrochim. Acta.* 23 (1978) 23.
31. Bentiss F., Traisnel M., Lagrenee M.,*Corros. Sci.* 42 (2000) 127.
32. Wu X., Ma S., Chen S., Xu Z., Sui A., *J. Electrochem. Soc.*146 (1999) 1847.
33. Ma H., Cheng X., Li G., Chen S., Quan Z., Zhao S., Niu L., *Corros .Sci.* 42 (2000) 1669.
34. Li P., Tan T.C., Lee T.Y.,*Corros.Sci.*38 (1996) 1935.
35. RehimS.S.A., HassanH.H., AminM.A.,*Appl. Surf. Sci.*189(2002) 279.
36. Kardas G., *J. Materials Science.* 41 (2005) 337.
37. Sastri V. S.,*Corrsion Inhibitors, John Wiley&Sons, New York,* (1998).
38. Do D., *Adsorption Analysis: Equilibria and Kinetics, Imperial College Press,* (1998).
39. Langmuir I., Am J.. *Chem. Soc.* 40 (1918) 1361.
40. Frumkin A.N., *Z. Phys. Chem.* 116 (1925) 466.
41. Hill T.L., *J. Chem. Phys.* 20 (1952) 141.
42. Boer J.H., *in: The Dynamical Character of Adsorption, Oxford University Press, Oxford,* 1953.
43. Parsons R., *J. Electroanal. Chem.* 8 (1964) 93.
44. Damaskin B.B., Petrii O.A., Batrakov V.V., *in: Adsorption of Organic Compounds on Electrodes, Plenum Press, New York,* 1971, p. 86, 94 and 247.
45. Kastening B., Holleck L., *Talanta*12 (1965) 1259.
46. Bockris J.O.M., Swinkels D.A.J., *J. Electrochem. Soc.* 111 (1964) 736.
47. El-Awady A.A., Abd-El-Nabey B.A., Aziz S.G., *J. Electrochem. Soc.* 139 (1992) 2149.
48. Rekkab S. , Zarrok H. , Salghi R., Zarrouk A., Bazzi Lh. , Hammouti B., Kabouche Z., Touzani R., Zougagh M., J. *Mater. Environ. Sci.* 3 (4) (2012) 613-627
49. Hukovic M. M., Baric R., Grubac Z., Brinic S., *J. Appl. Electrochem.*24 (1986) 772.
50. Caprioli F., Martinelli A., Di Castro V., Decker F., *J. Electroanal. Chem.* 693 (2013) 86.
51. Hong S., Chen W., Lao H.Q., Li N.B., *Corros. Sci.* 57 (2012) 270.
52. Popova A., Sokolova E., Raicheva S., Christov M., *Corros. Sci.* 45 (2003) 33.
53. Oguzie E.E., *Corros. Sci.* 50 (2008) 2993.
54. Oguzie E.E., Onuoha G.N., Onuchukwu A.L., *Mater. Chem. Phys.* 89 (2005) 305.

(2017) ; http://www.jmaterenvironsci.com/